

ACCEPTED MANUSCRIPT • OPEN ACCESS

Optical cuff for optogenetic control of the peripheral nervous system

To cite this article before publication: Frederic Michoud *et al* 2017 *J. Neural Eng.* in press <https://doi.org/10.1088/1741-2552/aa9126>

Manuscript version: Accepted Manuscript

Accepted Manuscript is “the version of the article accepted for publication including all changes made as a result of the peer review process, and which may also include the addition to the article by IOP Publishing of a header, an article ID, a cover sheet and/or an ‘Accepted Manuscript’ watermark, but excluding any other editing, typesetting or other changes made by IOP Publishing and/or its licensors”

This Accepted Manuscript is © 2017 IOP Publishing Ltd.

As the Version of Record of this article is going to be / has been published on a gold open access basis under a CC BY 3.0 licence, this Accepted Manuscript is available for reuse under a CC BY 3.0 licence immediately.

Everyone is permitted to use all or part of the original content in this article, provided that they adhere to all the terms of the licence <https://creativecommons.org/licenses/by/3.0>

Although reasonable endeavours have been taken to obtain all necessary permissions from third parties to include their copyrighted content within this article, their full citation and copyright line may not be present in this Accepted Manuscript version. Before using any content from this article, please refer to the Version of Record on IOPscience once published for full citation and copyright details, as permissions may be required. All third party content is fully copyright protected and is not published on a gold open access basis under a CC BY licence, unless that is specifically stated in the figure caption in the Version of Record.

View the [article online](#) for updates and enhancements.

Optical cuff for optogenetic control of the peripheral nervous system

Frédéric Michoud^{1,2,3}, Loïc Sottas^{1,2,3}, Liam E. Browne^{2,3,4}, Léonie Asboth⁵, Alban Latremolière^{2,3}, Miyuki Sakuma^{2,3}, Grégoire Courtine⁵, Clifford J. Woolf^{2,3} and Stéphanie P. Lacour^{1*}

¹ — Bertarelli Foundation Chair in Neuroprosthetic Technology, Laboratory for Soft Bioelectronics Interface, Institute of Microengineering, Institute of Bioengineering, Centre for Neuroprosthetics, Ecole Polytechnique Fédérale de Lausanne (EPFL), 1202 Geneva, Switzerland

² — Department of Neurobiology, Harvard Medical School, Boston, MA 02115, USA

³ — FM Kirby Neurobiology Center, Boston Children's Hospital, Boston, MA 02115, USA

⁴ — Wolfson Institute for Biomedical Research, University College London, London WC1E 6BT, UK

⁵ — International Paraplegic Foundation Chair in Spinal Cord Repair, Center for Neuroprosthetics and Brain Mind Institute, School of Life Sciences, Swiss Federal Institute of Technology (EPFL), 1202 Geneva, Switzerland.

Corresponding author (*): Stephanie.lacour@epfl.ch

Abstract

Objective. Nerves in the peripheral nervous system (PNS) contain axons with specific motor, somatosensory and autonomic functions. Optogenetics offers an efficient approach to selectively activate axons within the nerve. However, the heterogeneous nature of nerves and their tortuous route through the body create a challenging environment to reliably implant a light delivery interface. *Approach.* Here, we propose an optical peripheral nerve interface – an optocuff –, so that optogenetic modulation of peripheral nerves become possible in freely behaving mice. *Main results.* Using this optocuff, we demonstrate orderly recruitment of motor units with epineural optical stimulation of genetically targeted sciatic nerve axons, both in anaesthetized and in awake, freely behaving animals. Behavioural experiments and histology show the optocuff does not damage the nerve thus is suitable for long-term experiments. *Significance.* These results suggest that the soft optocuff might be a straightforward and efficient tool to support more extensive study of the PNS using optogenetics.

1. Introduction

Optical neural stimulation is emerging as an exciting and more advantageous alternative to traditional electrical stimulation. The conductive nature of biological tissue leads to electrical current spread, limiting spatial resolution and preventing cell-specific activation (Fenno et al., 2011, Warden et al., 2014). Genetic modification of neurons to express opsins, i.e. light-sensitive proteins on neuronal

1
2
3
4 membranes, renders neurons sensitive to light of a specific wavelength with millisecond precision
5 (Boyden et al., 2005). In the last decade, optogenetics has been used extensively to modulate neural
6 activity in the central nervous system (Deisseroth, 2015). In 2016, a human trial of optogenetics to
7 treat retinitis pigmentosa, a degenerative disease in which the specialized light-sensitive photoreceptor
8 cells in the eye die, was launched (clinicaltrials.gov # NCT02556736).

9
10 The use of optogenetics in the peripheral nervous system (PNS) has to date been relatively modest,
11 however, compared to optogenetic control in the brain (Montgomery et al., 2016, Jeschke and Moser,
12 2015), because of several physiologic and technological challenges. Peripheral nerves are complex,
13 heterogeneous tissues embedded in muscle and connective tissue, which strongly scatter and absorb
14 visible light. Nerves vary significantly in length and diameter, with small visceral nerves 100 times
15 smaller than larger nerves, such as the sciatic nerve. Peripheral nerve stimulation is often conducted in
16 awake, freely moving animals as anesthesia alters nerve excitability properties. Under normal
17 physiologic conditions, peripheral nerves are stretched as joints move and muscles elongate, making
18 consistent light delivery complex. Methods similar to those used in the brain can be used to express
19 opsins in peripheral neurons; however several groups have reported on the difficulties in doing so with
20 sufficient stability and efficacy and without interfering with the regular function of the peripheral
21 neurons (Miyashita et al., 2013).

22
23 Controlled and long-term light delivery to peripheral nerves requires advances in neurotechnology to
24 both enable long-lasting and efficient opsin expression in specific subsets of axons in peripheral
25 nerves and the production of implantable interfaces biointegrated with the flexible nerves and capable
26 of sufficient light power delivery over extended periods of time without producing nerve damage.

27
28 In a pioneer study, Llewellyn *et al.* demonstrated that optical stimulation of motor units in a nerve of a
29 transgenic mouse expressing the light-activated cation channel ChR2 in Thy1⁺ neurons better
30 approximated physiological recruitment of motor fibers than electrical stimulation (Llewellyn et al.,
31 2010). For the first time, this study presented an optoelectronic implant for optical modulation of the
32 sciatic nerve. However, the stiffness of the hybrid implant hosting 16 millimeter-side light emitting
33 diodes (LEDs) limited its application to acute, anaesthetized conditions only.

34
35 Transdermal optical stimulation is a non-invasive alternative approach to optogenetic stimulation of
36 peripheral sensory neurons. Excitation (Daou et al., 2013, Browne et al., 2017, Arcourt et al., 2017)
37 and inhibition (Iyer et al., 2014, Daou et al., 2016) of mouse primary afferent neurons have been
38 demonstrated using such a design but efficient control of axon activation strongly depends on the
39 optical properties of the intermediate tissues e.g. skin and subcutaneous tissue (Maimon et al., 2017,
40 Montgomery et al., 2016). Effectively, stimulation is limited to nerve terminals in the skin whose
41 superficial epidermal layers are innervated by nociceptors. Direct optical stimulation of nerves using
42 an implant is a promising approach for chronic PNS optogenetics. The question is how best to do this?

43
44 The rapidly expanding use of optogenetics in the CNS has triggered development of a variety of

1
2
3
4 optoprobes in the form of waveguide, miniaturized optical fibers and optoelectronic μ LED-based
5 arrays (Iseri and Kuzum, 2017, Fan and Li, 2015, Wu et al., 2013, Pisanello et al., 2017, Canales et al.,
6 2015, Alt et al., 2017) yet very few answer the technical needs for chronic peripheral nerve
7 optogenetics.
8

9
10 Inspired by the report from Towne *et al.* on an optical fiber-based nerve cuff for optical stimulation in
11 freely-behaving rats (Towne et al., 2013), we have constructed a soft and biointegrated optocuff as an
12 optical neural implant for chronic peripheral optogenetic stimulation in freely-behaving mice. The
13 optocuff delivers blue light to axons expressing channelrhodopsin (ChR2) in transgenic mice. We
14 overcame chronic implantation challenges with a miniaturized cuff design with soft materials and
15 motion-compliant optic fibers. We demonstrate optical muscle activation with epineural stimulation of
16 Thy1 expressing motor axons and a stable nerve-implant interface after 20 days *in vivo*. This optocuff
17 enables broad optogenetic neuromodulation of peripheral axons and is likely to contribute to the
18 evaluation of using this strategy for new therapeutic interventions for the impaired PNS.
19
20
21
22
23
24
25

26 **2. Methods**

27 *2.1. Mice*

28
29 All mice were purchased from Jackson Laboratories and Thy1-Cre mice were backcrossed to
30 C57BL/6 for at least 5 generations. Targeted expression of ChR2-tdTomato was achieved by breeding
31 heterozygous Rosa-CAG-LSL-hChR2(H134R)-tdTomato-WPRE (Ai27D) mice with Thy1-Cre mice.
32 Resultant Thy1-Cre::ChR2 mice were heterozygous for both transgenes and were housed with control
33 littermates. Mice were given *ad libitum* access to food and water and were housed in at $22 \pm 1^\circ\text{C}$, 50%
34 relative humidity, and a 12-hr light:12-hr dark cycle. Male and female mice were pooled by genotype
35 to limit the number of animals used. All experiments were conducted according to institutional animal
36 care and safety guidelines and with IACUC approval at Boston Children's Hospital, and accordance
37 with Swiss federal legislation and under the guidelines established at EPFL and approved by local
38 Swiss Veterinary Offices.
39
40
41
42
43
44
45
46
47

48 *2.2. DRG neuron culture and electrophysiology*

49
50 Dorsal root ganglia neurons were isolated from adult (3-6 month old) mice and maintained at 37°C in
51 5% carbon dioxide. Electrophysiological recordings were made at $20\text{--}22^\circ\text{C}$ up to 24 h after DRG
52 neuron dissociation, using the whole-cell configuration of the patch-clamp technique. Recording
53 pipettes had tip resistances of $4\text{--}8\text{ M}\Omega$ when filled with (in mM): 135 K-gluconate, 10 KCl, 1 MgCl_2 ,
54 5 EGTA, and 10 HEPES, pH 7.3. The extracellular solution contained (in mM): 145 NaCl, 5 KCl, 2
55 CaCl_2 , 1 MgCl_2 , 10 HEPES, and 10 glucose, pH 7.4. All solutions were maintained at $300\text{--}315$
56 mOsm/l. Membrane potential was recorded in current clamp mode with an Axopatch 200A amplifier
57 and Digidata 1400A A/D interface using pClamp 10.2 software (Molecular Devices). The data were
58
59
60

1
2
3
4 low-pass filtered at 5 kHz (4-pole Bessel filter) and sampled at 10 kHz. Input resistance was typically
5 >500 M Ω , and cells with resistances <200 M Ω were discarded. Care was taken to maintain membrane
6 access resistance as low as possible (usually 3–7 M Ω and always less than 10 M Ω). Detailed methods
7 can be found in (Browne et al., 2017).
8
9

10 11 12 13 2.3. Nerve optical properties

14 Sciatic nerves of 5 naïve adult mice were carefully explanted after CO₂ asphyxiation, immersed in
15 PBS then embedded in 2.5% agarose gel. Cross-sectional slices (100-1000 μm thick) were obtained
16 with a vibratome apparatus (VTS1200, Leica) and mounted on microscopic glass slides (Superfrost,
17 Thermo Scientific). A drop of saline was added to prevent slices from drying. Tissue transmittance
18 was immediately measured with an optical system composed of a photodiode (S170C, Thorlabs), a
19 power meter console (PM100D, Thorlabs) and a 473 nm DPSS laser (100 mW, LaserGlow) coupled to
20 a multimode SMA optic fiber (105 μm core diameter, 1 m length, Thorlabs). The sensor was shaded
21 with a mask matching nerve cross-section dimensions and a constant intensity (15 mW.mm⁻²)
22 illuminated the slices. The light radial distribution in sciatic nerve tissue was finally modeled using the
23 modified 1D Beer-Lambert law:
24
25
26
27
28
29

$$30 \quad I(z) = I_0 * e^{(-\mu_{eff} * z)}$$

31
32
33
34 where I_0 is the optic fiber output irradiance, μ_{eff} the effective attenuation coefficient and z the slice
35 thickness (Al-Juboori et al., 2013).
36
37
38

39 2.4. Optocuff construction

40 The cuff was built upon a polystyrene rod template (0.88 mm diameter, Evergreen). A soft 150 μm
41 thick platinum-catalyzed silicone (Ecoflex 00-50, Smooth-On) was vertically spin-coated and cured (2
42 h at 80 °C). A gold film was sputtered (80 nm, DP650, Alliance Concept) on the silicone to act as a
43 light reflective coating. Finally, a micrometric film of Polydimethylsiloxane (PDMS) (Sylgard 184,
44 Dow Corning) was used for encapsulation by spray deposition of a PDMS–Heptane mixture. A 12 cm
45 optic fiber (FG105UCA, 105 μm inner core diameter Thorlabs) was processed similarly to previous
46 papers (Sparta et al., 2011). Briefly, the acrylate coating tip-end of the fiber was dissolved in acetone
47 and terminated with a 1.25 mm ceramic ferrule (CFLC128, Thorlabs). The fiber was then polished
48 using a dedicated kit (Thorlabs) and its light transmission controlled with a power sensor. The distal
49 end of the fiber was perpendicularly coupled to the cuff template and polymer sealed (Kwik-Sil,
50 World Precision Instruments). Finally, the rod was carefully removed, the cuff trimmed (2 mm length,
51 0.8 mm inner diameter) and a sharp incision was applied transversally to the cuff. The compressive
52 stress built during elastomer curing caused the cuff to spontaneously fold spirally.
53
54
55
56
57
58
59
60

2. 5. *Optocuff implantation*

All animal procedures were approved by the institutional animal care and safety guidelines and with IACUC approval at Boston Children's Hospital. Healthy adult (3-6 month old) male and female Thy1-Cre::ChR2 mice of average mass 27.5 g were implanted with the optical cuff. Mice were anesthetized under isoflurane (1–3%) and the body temperature was maintained with a heated surgical table (37 °C). The left hindlimb and head of the mouse were shaved and the skin disinfected using successive applications of betadine and isopropyl alcohol. Under sterile conditions, a skin incision exposed the skull, where 2 precision screws were drilled. The sciatic nerve was exposed at the mid-thigh level after a parallel 1 cm long skin incision and blunt muscles separation. The optical cuff and optic fiber were threaded subcutaneously, the ferrule end laying down the mouse skull and the cuff proximal to the sciatic nerve. A loop was formed on the optic fiber so the cuff has a 90 ° incidence angle on the sciatic nerve and to relieve the strain along the fiber after implantation. The cuff was then applied to wrap the sciatic nerve and a loose suture secured the optic fiber to surrounding muscles. The separated muscles were sewed back together with absorbable sutures. The ferrule was anchored to the skull with a small amount of dental cement, and the incisions at the head and hindlimb closed with sutures (6-0, Ethicon). Full surgical procedure took 45 minutes. Control mice used in behavioural experiments underwent similar surgical procedure with the skull and sciatic nerve being exposed. Only a ferrule fixed on a 1 cm long optic fiber was mounted on the skull so blinded experimenters could not distinguished experimental groups. Mice were allowed to recover in single housed cage and subcutaneously injected with post-operative meloxicam analgesic for 3 days.

2. 6. *EMG electrode implantation and data acquisition*

All surgical procedures were performed in accordance with Swiss federal legislation and under the guidelines established at EPFL and approved by local Swiss Veterinary Offices. The animals were administered general anesthesia (mixture of 80 mg/ml ketamine, 10 mg/ml xylazine, diluted in saline), using intraperitoneal injections (8.5 ml/kg). Bipolar intramuscular electrodes (AS632, Cooner Wire) were inserted unilaterally in the tibialis anterior (TA, ankle flexor) muscles to record electromyographic activity. Recording electrodes were created prior to implantation by removing a small part (~200 μ m notch) of Teflon insulation. All the wires were connected to a percutaneous amphenol connector (Omnetics Connector Corporation). EMG recordings were synchronized with the laser stimulation onset using a custom-developed Tucker-Davis Technology (TDT) code. Signals were amplified (x1000) and pre-filtered (Bandpass: 100 Hz -1 kHz) with an AM systems amplifier.

2. 7. *Optogenetic control and high-speed behavioural imaging*

The optical cuff was coupled to the laser with a multimode FC/PC optic fiber cable (105 μ m core diameter, 2 m length, Thorlabs) using a ceramic mating sleeve (ADAL1, Thorlabs) on the ferrule. It

1
2
3
4 was critical avoiding any physical stress on the mouse during the operation. Mice were housed in a
5 small chamber (7.5 x 7.5 x 15 cm³) chambers and acclimatized for at least 30 minutes. A counter-
6 balance lever arm (Harvard Apparatus) relieved the mouse from the laser optic fiber cable weight. A
7 computer-controlled pulse generator (OPTG-4, Doric) was used to supply TTL signals to the laser
8 driver. Simultaneous epineural optogenetic stimulation (average 40 mW laser output) and high-speed
9 recordings were performed. Behaviour was sampled at 1000 frames per second using an acA2040-
10 180kmNIR cameralink CMOS camera (Basler) with a 8 mm lens and set at 500 pixels x 350 pixels.
11 Acquisition was carried out in LabVIEW on a computer with excess buffer capacity to ensure all
12 frames were successfully retained. Littermate control mice without Cre recombinase and implanted
13 with the optical cuff did not react to blue light pulse (20 ms, 60 mW). Cuff implanted Thy1-Cre::ChR2
14 mice did not respond to an equivalent off-spectra pulse of light (594 nm, LaserGlow).
15
16
17
18
19
20
21
22

23 2. 8. Behavioral experiments

24 All experiments were conducted in a quiet room at 22 ± 1°C with 50% relative humidity. Animals
25 were acclimatized to the behavioral testing apparatus during three habituation sessions in advance of
26 starting the experiment. The behavioral tester was blinded until the experiment was complete.
27
28
29
30

31 2. 8. 1. Mechanical sensitivity

32 Mice were habituated, single housed in a small transparent chamber (7.5 x 7.5 x 15 cm³) elevated on a
33 wire grid. Mechanical sensitivity was measured by applying an increasing perpendicular force to the
34 lateral plantar surface of the left hindpaw using graded series of six von Frey filaments (with bending
35 force of 0.04, 0.07, 0.16, 0.4, 0.6, 1 g) and counting the number of withdrawal responses across ten
36 applications. The pain mechanical threshold was defined as the minimal force triggering at least 5
37 withdrawals.
38
39
40
41
42
43

44 2. 8. 2. Thermal sensitivity

45 Each mouse was habituated on a warmed (29 °C) glass platform of a Hargreave's apparatus (IITC Life
46 Science). Thermal sensitivity was determined by applying a radiant heat source to the plantar hindpaw
47 while measuring the duration before hindpaw withdrawal. The latency for the onset of nocifensive
48 behavior was timed. This latency was determined 3 times per animal, per session, with a 5 minutes
49 interval to prevent thermal sensitization.
50
51
52
53
54
55

56 2. 8. 3. Dynamic weight bearing

57 Mice inflammatory pain was assessed using a DWB test (Bioseb). Each mouse was placed 5 minutes
58 in a Plexiglas chamber (11 x 19.7 x 11 cm³) with a pressure transducers array on the floor. A camera
59 recorded each movement while the mouse was exploring the chamber. Using a software matching
60

1
2
3
4 pressure data and the video recordings, we discriminated and measured the weight (in grams) applied
5 by the limbs. Finally, we extracted the duration of the cuff implanted hindpaw on the floor over the
6 contralateral one.
7
8
9

10 2. 8. 4. *Motor sciatic nerve assessment*

11 Motor recovery in mice was assessed using a DigiGait apparatus (Mouse Specifics). Mice were
12 recorded walking on the treadmill videography system at 20cm/s. Measures of toe spread (TS) and the
13 print length (PL, distance of the 3rd toe tip to the most posterior paw part) were used to calculate the
14 sciatic nerve functional index (SFI) using the following formula (Baptista et al., 2007):
15
16
17

$$18 \quad SFI = 118.9 * \frac{(TS_{left} - TS_{right})}{TS_{right}} - 51.2 * \frac{(PL_{left} - PL_{right})}{PL_{right}} - 7.5$$

19
20
21
22
23
24

25 2. 9. *Tissue preparation and fluorescence imaging*

26 Mice were anesthetized with pentobarbital (100 mg.kg⁻¹ intraperitoneal) and fixed by transcardial
27 perfusion with 4% paraformaldehyde dissolved in phosphate buffered saline (PBS). DRG (L3-L5) and
28 sciatic nerves were dissected, postfixed, washed, cryoprotected with sucrose in PBS (30% w/v) for 2-3
29 days, and frozen (O.C.T., Tissue-Tek). Cryosections of DRG (10 μm thick) and sciatic nerves (10 μm
30 longitudinal sections, 10 μm cross-sections) were blocked with 1% bovine albumin serum (BSA) and
31 0.1% triton X-100 in PBS for one hour. Sections were incubated with NF200 (1:2000), CGRP (1:500)
32 primary antibody in fresh blocking solution overnight at 4°C and washed three times (10 minutes
33 each) in saline. They were then incubated with secondary IgG antibody (1:500, Life Technologies) for
34 one hour at room temperature, washed three times (10 minutes each) in PBS, and mounted in
35 Vectashield (H-1200). Fluorescein-conjugated GSL I was used at 1:1000. Finally, sciatic nerve cross-
36 sections were incubated with DAPI (1:1000, 15 minutes, Sigma) and washed in PBS. DRG and sciatic
37 nerve sections were imaged using a Nikon Eclipse 80i microscope using a Nikon 10X objective and
38 Nikon DS-Qi1MC camera. In DRG and sciatic nerves, fluorescence corresponding to tdTomato was
39 absent in tissues from littermate mice that did not express ChR2-tdTomato or that did not express the
40 Cre recombinase
41
42
43
44
45
46
47
48
49
50
51
52

53 3. Results

54 3. 1. *Functional expression of ChR2 in the PNS*

55 The light-activated ion channel ChR2 was expressed in a broad class of sensory and motor neurons
56 using a Cre-recombinase transgenic approach (Campsall et al., 2002); Cre-dependent ChR2-tdTomato
57 mice were crossed with Thy1-Cre driver mice. The resultant Thy1-Cre::ChR2 mice were heterozygous
58 for both transgenes and ChR2 was found in dorsal root ganglion (DRG) neurons and in sciatic nerve
59
60

axons (fig. 1 A, B). Of the ChR2+ DRG neurons, 41% were myelinated (NF200), 4% were CGRP+ and 5% IB4+. Electrophysiological studies using whole-cell current clamp recordings from ChR2-tdTomato+ DRG neurons showed action potentials were elicited by light (fig. 1 C). The large range of membrane capacitances ([11 – 51] pF; mean 28 ± 4 pF) and thresholds ([-56 – -35] mV; mean -44 ± 2 mV) indicate a broad neuron population was targeted (Browne et al., 2017), as expected for the Thy1 promoter. Functional expression of ChR2 at the mid-axon enables an epineural light-delivery strategy.

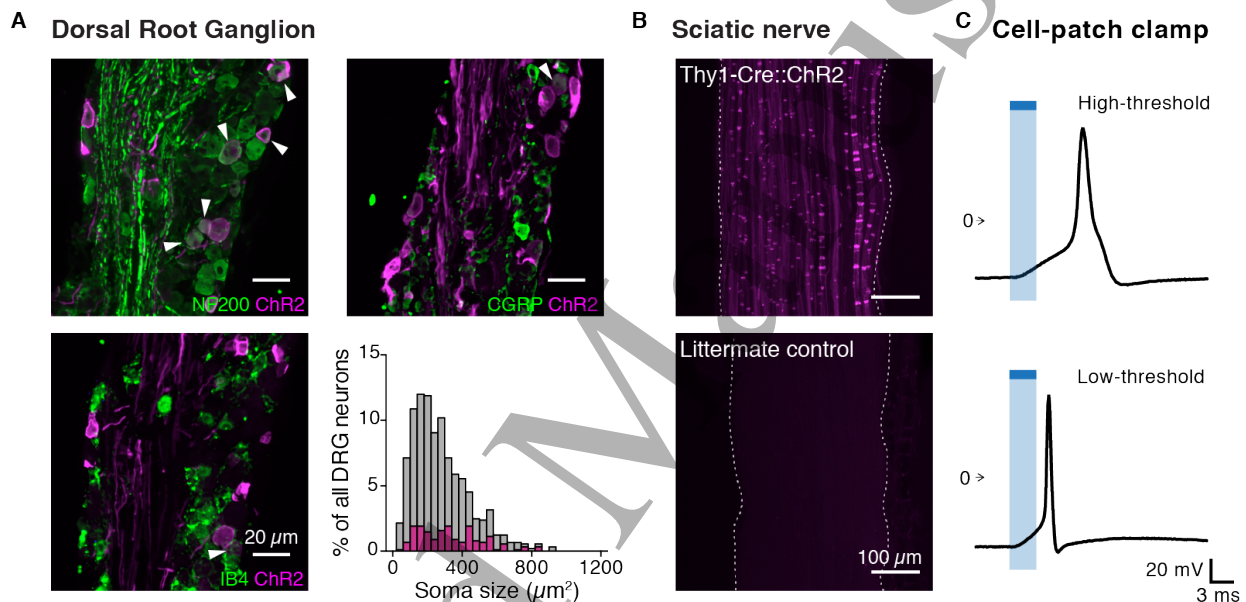


Figure 1: Expression of ChR2 in the PNS of Thy1-Cre::ChR2+ mice. A) Expression of ChR2-tdTomato in DRG soma was found in a broad class of neurons, myelinated (NF200+, top left), CGRP+ (top right) and IB4+ (bottom left). White arrows indicate overlapping fluorescence emitting neurons. Scale bar 20 μ m. ChR2 was expressed in a wide range of cell sizes as estimated using NeuN+ as a marker for all neurons (bottom right). B) Expression of ChR2-tdTomato in sciatic nerve fibers. Scale bar 100 μ m. Fluorescence was not observed in any of the littermate controls. C) Whole-cell current clamp recordings of action potentials elicited by light in cultured ChR2-tdTomato+ DRG neurons (17 neurons, 3 mice). These cells displayed a wide range of membrane capacitances and thresholds. Neurons from littermate controls did not show any effect of light (6 neurons). Light (473 nm for 3 ms) applied at 6 mW.mm⁻².

3. 2. A mouse soft, implantable optical cuff

We designed the optocuff as a soft, tubular construct that can be delicately wrapped around a mouse peripheral nerve, e.g. the sciatic nerve (fig. 2 A). Light is delivered to the cuff and the nerve via a flexible optic fiber (105 μm core) subcutaneously threaded from a miniaturized headstage and anchored to the cuff. Multilayers of soft silicones (25kPa Young's modulus) coated with a reflective thin gold film and a final PDMS film form the 2 mm long, 1 mm diameter cuff (fig. 2 B). The reflective metallic coating limits light spill to the surrounding tissues. The soft implant does not compress nor hinder the natural movement of the nerve as its elasticity surpasses that of the nerve (fig. 2 C).

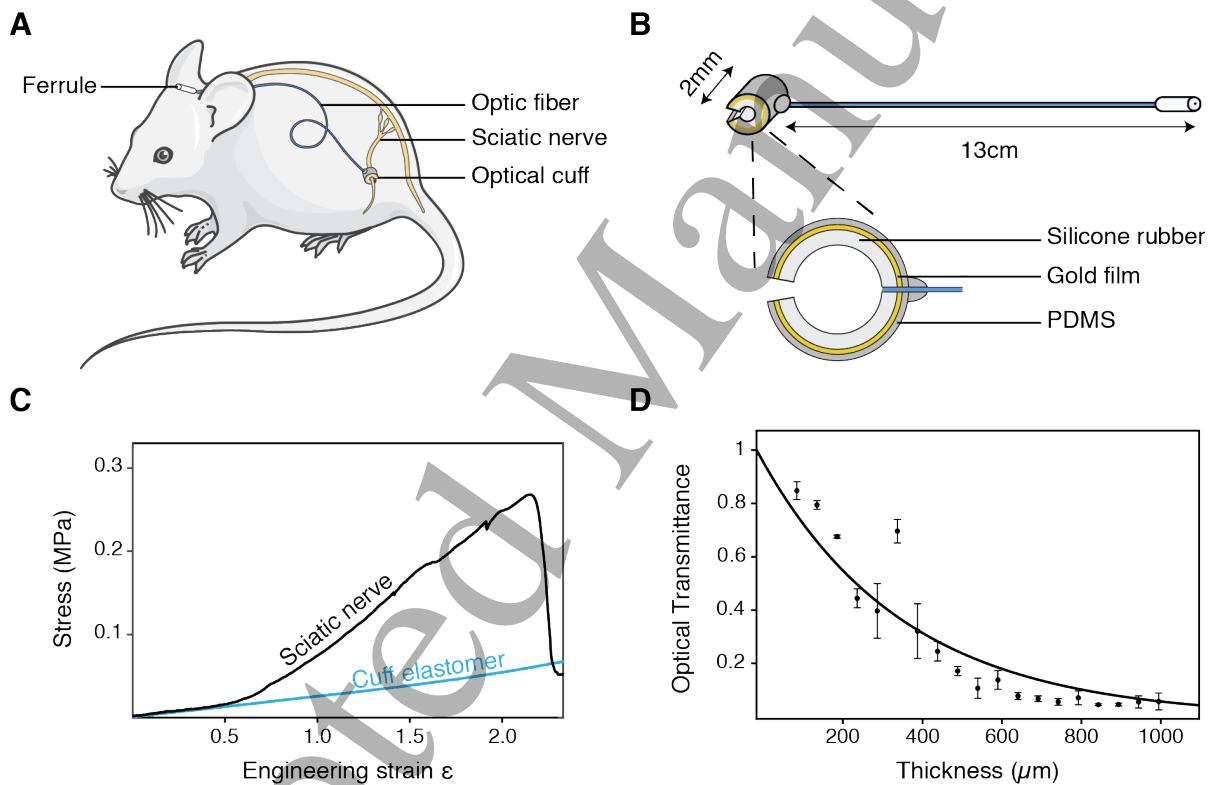


Figure 2: Experimental system for optogenetic activation of the mouse PNS. A) Optical stimulation carried out epineurally in Thy1-Cre::ChR2 mice implanted with an optocuff. B) Optical cuff illustration. A thin flexible optic fiber terminates on a silicone rubber-based cuff to deliver an optical stimulation on the mouse sciatic nerve. A gold thin film enables light to reflect internally. C) Tensile strain-stress curves recorded from a fresh sciatic nerve immersed in physiological conditions and from the elastomeric cuff ($n = 1$ per group). D) Relative optical power transmission at 473 nm through fresh dissected sciatic nerve tissue ($n = 4$ per thickness).

1
2
3
4 We measured blue light transmission *in vitro* through slices of freshly dissected sciatic nerves. Light
5 is rapidly absorbed with an effective attenuation coefficient μ_{eff} of 3.503 mm^{-1} at 473 nm tissues (fig. 2
6 D). We measured an average of 16% optical power losses from the optic fiber to the optocuff such
7 that sufficient light power can be delivered at the optocuff to excite opsin-carrying axons. Heating
8 within the optocuff is limited to photon absorption, a significant advantage compared to LED-based
9 optoelectronic interfaces at analogous optical power (Yizhar et al., 2011).
10
11
12
13
14

15 16 3.3. Orderly muscle recruitment to optical stimulation

17 To measure electromyographic (EMG) responses of anaesthetized Thy1::ChR2 mice to peripheral
18 optical stimulation of motor axons the sciatic nerve of the mouse was exposed and implanted with the
19 optocuff under general anesthesia (fig. 3 A). Then, thin EMG electrodes were inserted into the
20 ipsilateral tibialis anterior (TA), an ankle flexor muscle innervated by the peroneal branch of the
21 sciatic nerve. EMG recordings were synchronized with optical stimulation generated by an external
22 473 nm laser. Short pulses of light consistently triggered unilateral TA contractions, resulting in light-
23 activated twitches. We characterized the muscle recruitment with the peak-to-peak value of EMG
24 signal in the early phase of the response. We found the muscle fibers were recruited in an orderly
25 fashion with the power of epineural irradiance of the optical stimulation (fig. 3 B, C). These results
26 suggest more motor units were recruited with higher irradiance stimulation, consequently inducing
27 larger muscle responses. Latency for the EMG onset (mean 6.1 ± 0.3 ms, 60 trials, 10 ms pulse width)
28 was stable relative to the optical stimulation intensity and peak-to-peak amplitude (mean 6.1 ± 0.25
29 mV), implying direct activation of large and fast motor axons. The TA EMG amplitude directly
30 correlated with optical pulse width (fig. 3 D), indicating an increased activation of motor neurons with
31 longer pulses. These results demonstrate peripheral optogenetic modulation in anesthetized mice with
32 the optocuff.
33
34
35
36
37
38
39
40
41
42

43 Next, we tested if the soft optocuff affects the sciatic nerve over time. We implanted a group of Thy1-
44 Cre::ChR2 mice for 20 days with an optocuff wrapped around the left sciatic nerve; one end of the
45 optic fiber was permanently anchored to its head-mounted ferrule. Histological cross-section of the
46 nerve at the cuff site did not show any sign of demyelination or signs of inflammation after the
47 prolonged implantation (fig. 4 A, B). Coherent with this, sensory and motor behavioral assessments
48 did not reveal any change at various times after implantation. Thermal and mechanical pain-related
49 assays as well as weight bearing and gait were conducted prior and after surgery and did not reveal
50 any significant change ($p > 0.05$, ANOVA with Dunnett's method)
51
52
53
54
55
56
57
58
59
60

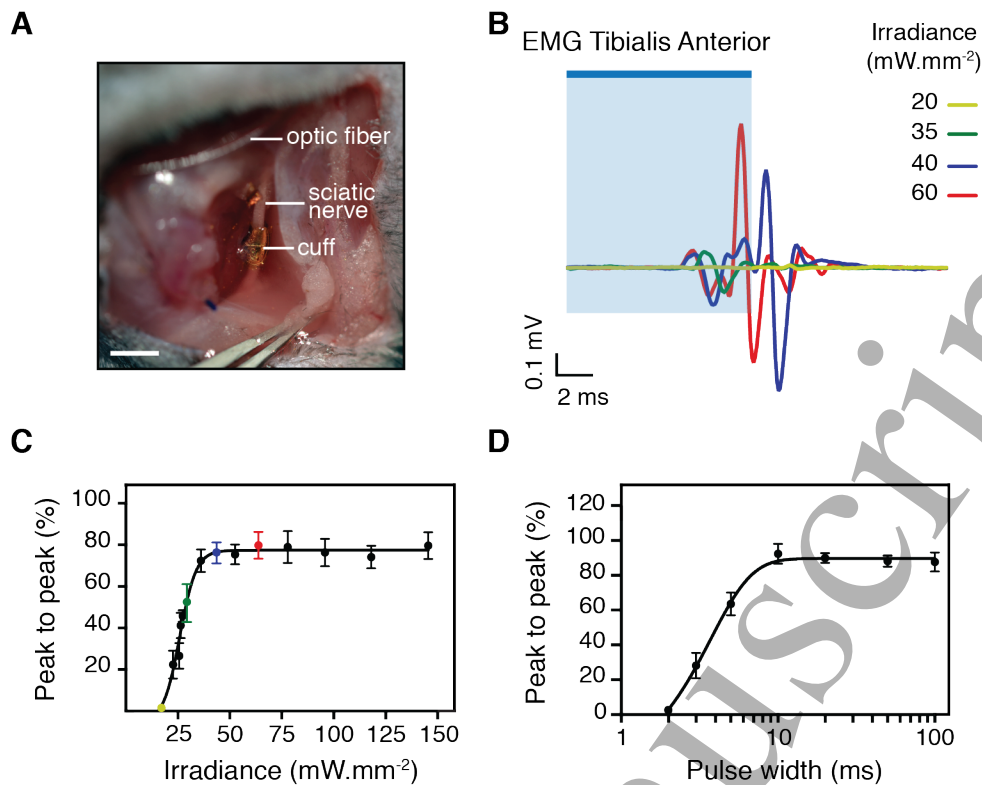


Figure 3: Optical stimulation of the sciatic nerve in anaesthetized mice. A) Optocuff implantation on the sciatic nerve. Scale bar 2 mm. B-D, Optogenetic stimulation of peripheral axons in anaesthetized Thy1-Cre::ChR2 mice. Light-activated Tibialis Anterior EMG at various stimulation irradiances. The threshold for muscle contraction was 25 mW.mm⁻² (B). The blue bar indicates the stimulation duration (10ms). EMG amplitude is directly correlated with stimulation irradiance (C) and pulse width (D). (n = 3 Thy1-Cre::ChR2 mice, 5 trials per condition; irradiance set at 60 mW.mm⁻²).

3.4. Epineural stimulation of motor neuron axons in awake mice

Next, we tested whether the optocuff could reliably deliver epineural optical stimulation in awake, freely-behaving mice. We applied epineurally short (2-100 ms) light pulses at 473 nm with the optocuff while continuously monitoring the behavior of Thy1-Cre::ChR2 mice at 1kHz with a camera (Basler Ace acA2040-180km). Optogenetic stimulation of the Thy1 axons resulted in short latency hindlimb muscle contraction (fig. 5 A, B, Supp. V1). We observed global limb extension and paw opening with short (> 5 ms) blue illumination. Probability of behavioural response to optical stimulation was higher with longer pulses (fig. 5 C) and reached 100% for pulses longer than 20 ms. We found the delay for the change in behavior elicited by epineural stimulation was stable through different effective pulse duration (mean 17.9 ± 0.58 ms, fig. 5 D). Using conduction velocity analysis, we concluded these changes in behavior were elicited by direct activation of motor neurons (Steffens et al., 2012).

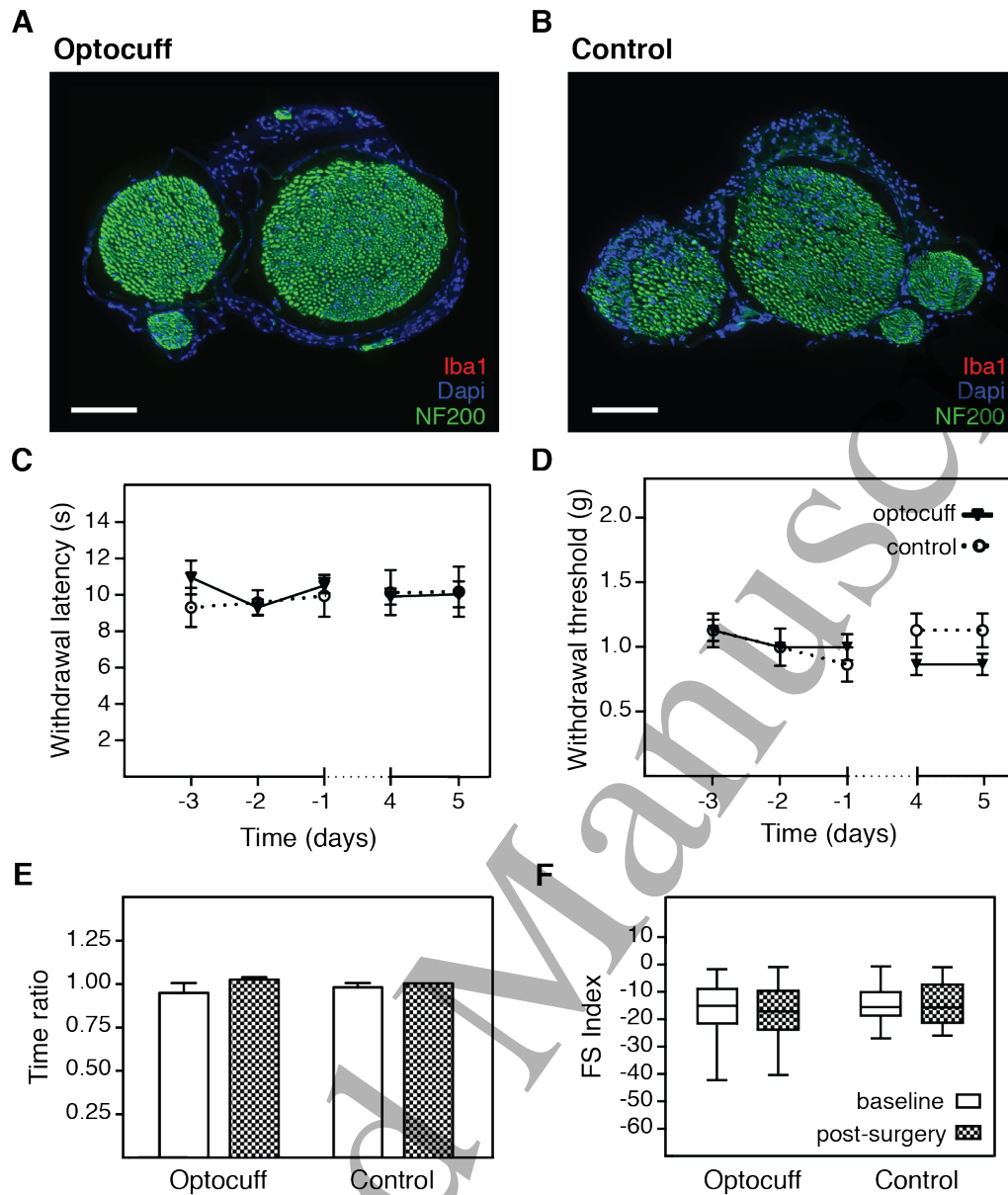


Figure 4: Histology and behavioural experiments reveals the optocuff is suitable for long-term implantation. A-B, Sciatic nerve cross-sectional images 20 days following cuff implantation (A) or sham surgery (B). C-D, Thermal (C) and Mechanical (D) sensitivity assessed with Hargreaves and von Frey respectively, in cuff implanted ($n = 6$) and control groups ($n=3$). Surgery was performed on day 0. E) Dynamic weight bearing analysis of the duration of time spent on the ipsilateral versus the contralateral hindpaw, before surgery (white) and 5 days post-surgery (optocuff implantation) (grey). F) Box plot representation of the functional sciatic index calculated gait analysis on treadmill (20 cm/s).

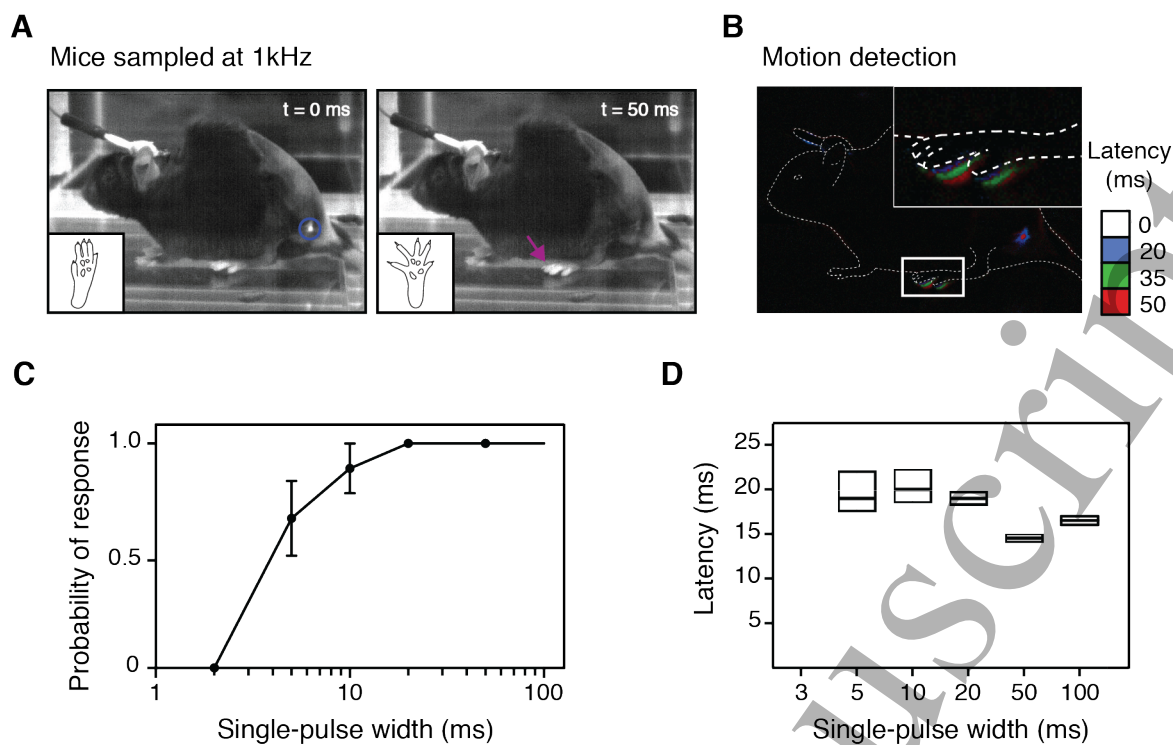


Figure 5: Optogenetic control of peripheral neurons in awake behaving mice. A) Behaviour sampled at 1 kHz elicited by a single pulse of light (50 ms, 40 mW.mm²) applied to the sciatic nerve using the optocuff. Onset of the optical stimulation can be seen transdermally. Epineural optical stimulation of Thy1 axons in the sciatic nerve results in hindlimb muscle contraction and paw opening. B) Motion detection reveals the kinetics of this behaviour. The latency to the response was 17 ms (**Supplementary video V1**). This analysis was conducted by comparing the difference in pixel intensity between frames. C) Probability of behavioural response to an epineural optogenetic stimulus depends on the pulse width (n = 3 mice, 5 trials per condition). D) Response latency upon epineural activation of Thy1 neurons demonstrates more stability with longer pulses. The mean latency did not depend on pulse duration (n = 3 Thy1-Cre::ChR2+ mice, 5 trials per condition). Littermate control cuff implanted mice did not show any response to light stimuli.

Furthermore, absence of response to optical stimulation carried with the optocuff in control littermate mice implies that light-responses were not caused by heat or visual artifact.

4. Discussion

We have developed an implantable optical interface that enables optogenetic modulation of the PNS in freely-behaving small animals such as mice. The soft optocuff can be wrapped around the sciatic nerve inducing minimal foreign body reaction. Using transgenic Thy1-Cre::ChR2 mice, direct and robust muscle activation was obtained by optical stimulation of axons in the sciatic nerve, both in

1
2
3
4 anaesthetized and awake animals. The muscular response can be finely tuned with the optical
5 stimulation parameters i.e. pulse width and irradiance.
6

7
8
9 Stable light delivery to neurons/axons *in vivo* has been challenging, particularly for applications in the
10 spinal cord or peripheral nerves (Montgomery et al., 2016). The relative motion of these soft
11 biological tissues prevent long-term and reliable interface with the stiff implants. Although studies
12 have bypassed this problem by stimulating nerve-endings via transdermal illumination (Daou et al.,
13 2013, Iyer et al., 2014, Arcourt et al., 2017, Browne et al., 2017) or using implanted wireless LEDs
14 (Montgomery et al., 2015, Park et al., 2015), interfacing the whole nerve directly offers a broad range
15 of opportunities. We find that reducing the mechanical mismatch between the nerve and implant and
16 optimizing the surgical procedure were key for successful long-term optical coupling with the mouse
17 PNS. The system relies on compliant, subcutaneously tethered fibers that enable a higher intensity and
18 thermally safer light stimulation compared to optoelectronic systems. Additionally, the commercially
19 available external light-sources allow for a large range of solutions for future optogenetic experiments.
20 Opsin expression in the mouse PNS was achieved using the transgenesis route. Although recent
21 studies have exploited optogenetics in rats or primates (L et al., 2017, Pawela et al., 2016, Klein et al.,
22 2016), mice are still the predominant species used in the neurobiology field. This animal model
23 presents obvious advantages for genetic manipulations, resulting in a large number of Cre-lines and
24 Cre-dependent viral vectors available. We show that Chr2 opsin expression in PNS neurons was
25 robust enough for optical modulation *in vitro* and *in vivo*. The optocuff system can be used for a wide
26 variety of optogenetic experimental approaches, including activation as here and neural inhibition with
27 opsins such as halorhodopsin (NpHr) or archaerhodopsin (Arch). Multi-spectra modulation using
28 multimodal optic fibers will further broaden opportunities for the soft optocuff system (Chuong et al.,
29 2014, Berndt et al., 2014).
30

31
32
33 Finally, long-term selective modulation of the PNS by light delivery offers new experimental
34 opportunities. Optical stimulation of peripheral axons has great implications for muscle control and
35 nerve regeneration (Bryson et al., 2014, Liske et al., 2013), for the study of sensory biology (Browne
36 et al., 2017) and for autonomic output (Kim et al., 2015). Similarly, optogenetic inhibition *in vivo* will
37 enable to tease out the functional role of specific neurons involve in complex disease mechanisms,
38 such as tactile allodynia following nerve injury (Daou et al., 2016).
39

40
41
42 In summary, soft optocuffs are a simple and efficient tool to probe the PNS with optogenetics. Its
43 manufacturing does not require extensive microfabrication processes. Further miniaturization and
44 addition of a wireless head-mounted light source would allow for an even broader use of the implant,
45 especially to study smaller nerves, such as autonomic and visceral nerves (Birmingham et al., 2014).
46

47
48
49 Finally, the optocuff system supports optogenetics as a versatile tool to unravel the PNS function, an
50 essential step with therapeutic outcomes in many diseases, such as chronic pain.
51
52
53
54
55
56
57
58
59
60

Acknowledgments

The authors would like to thank I. Minev for advices on the soft cuff fabrication, N. Andrews for the animal facility management, L. Barrett for the laboratory management and G. Gorski for his help with histology. Finally, authors would like to thank the EPFL Center for Micronanotechnology (CMi) staff for their technical support. This work is supported by the Swiss National Science Foundation, grant BSCGIO_157800, the Bertarelli Foundation and the European Commission, 329202. The authors have no competing interests to disclose.

References and Notes

- AL-JUBOORI, S. I., DONDZILLO, A., STUBBLEFIELD, E. A., FELSEN, G., LEI, T. C. & KLUG, A. 2013. Light scattering properties vary across different regions of the adult mouse brain. *PLoS One*, 8, e67626.
- ALT, M. T., FIEDLER, E., RUDMANN, L., ORDONEZ, J. S., RUTHER, P. & STIEGLITZ, T. 2017. Let There Be Light-Optoprobes for Neural Implants. *Proceedings of the IEEE*, 105, 101-138.
- ARCOURT, A., GORHAM, L., DHANDAPANI, R., PRATO, V., TABERNER, F. J., WENDE, H., GANGADHARAN, V., BIRCHMEIER, C., HEPPENSTALL, P. A. & LECHNER, S. G. 2017. Touch Receptor-Derived Sensory Information Alleviates Acute Pain Signaling and Fine-Tunes Nociceptive Reflex Coordination. *Neuron*, 93, 179-193.
- BAPTISTA, A. F., GOMES, J. R., OLIVEIRA, J. T., SANTOS, S. M., VANNIER-SANTOS, M. A. & MARTINEZ, A. M. 2007. A new approach to assess function after sciatic nerve lesion in the mouse - adaptation of the sciatic static index. *J Neurosci Methods*, 161, 259-64.
- BERNDT, A., LEE, S. Y., RAMAKRISHNAN, C. & DEISSEROTH, K. 2014. Structure-guided transformation of channelrhodopsin into a light-activated chloride channel. *Science*, 344, 420-4.
- BIRMINGHAM, K., GRADINARU, V., ANIKEEVA, P., GRILL, W. M., PIKOV, V., MCLAUGHLIN, B., PASRICHA, P., WEBER, D., LUDWIG, K. & FAMM, K. 2014. Bioelectronic medicines: a research roadmap. *Nat Rev Drug Discov*, 13, 399-400.
- BOYDEN, E. S., ZHANG, F., BAMBERG, E., NAGEL, G. & DEISSEROTH, K. 2005. Millisecond-timescale, genetically targeted optical control of neural activity. *Nat Neurosci*, 8, 1263-8.
- BROWNE, L. E., LATREMOLIERE, A., LEHNERT, B. P., GRANTHAM, A., WARD, C., ALEXANDRE, C., COSTIGAN, M., MICHOD, F., ROBERSON, D. P., GINTY, D. D. & WOOLF, C. J. 2017. Time-Resolved Fast Mammalian Behavior Reveals the Complexity of Protective Pain Responses. *Cell Rep*, 20, 89-98.
- BRYSON, J. B., MACHADO, C. B., CROSSLEY, M., STEVENSON, D., BROS-FACER, V., BURRONE, J., GREENSMITH, L. & LIEBERAM, I. 2014. Optical control of muscle function by transplantation of stem cell-derived motor neurons in mice. *Science*, 344, 94-7.
- CAMPALL, K. D., MAZEROLLE, C. J., DE REPENTINGY, Y., KOTHARY, R. & WALLACE, V. A. 2002. Characterization of transgene expression and Cre recombinase activity in a panel of Thy-1 promoter-Cre transgenic mice. *Dev Dyn*, 224, 135-43.
- CANALES, A., JIA, X., FRORIEP, U. P., KOPPE, R. A., TRINGIDES, C. M., SELVIDGE, J., LU, C., HOU, C., WEI, L., FINK, Y. & ANIKEEVA, P. 2015. Multifunctional fibers for simultaneous optical, electrical and chemical interrogation of neural circuits in vivo. *Nat Biotechnol*, 33, 277-84.
- CHUONG, A. S., MIRI, M. L., BUSSKAMP, V., MATTHEWS, G. A., ACKER, L. C., SORENSEN, A. T., YOUNG, A., KLAPOETKE, N. C., HENNINGER, M. A., KODANDARAMAIAH, S. B., OGAWA, M., RAMANLAL, S. B., BANDLER, R. C., ALLEN, B. D., FOREST, C. R., CHOW, B. Y., HAN, X., LIN, Y., TYE, K. M., ROSKA, B., CARDIN, J. A. & BOYDEN, E. S. 2014. Noninvasive optical inhibition with a red-shifted microbial rhodopsin. *Nat Neurosci*, 17, 1123-9.
- DAOU, I., BEAUDRY, H., ASE, A. R., WIESKOPF, J. S., RIBEIRO-DA-SILVA, A., MOGIL, J. S. & SEGUELA, P. 2016. Optogenetic Silencing of Nav1.8-Positive Afferents Alleviates Inflammatory and Neuropathic Pain. *eNeuro*, 3.

- 1
2
3
4 DAOU, I., TUTTLE, A. H., LONGO, G., WIESKOPF, J. S., BONIN, R. P., ASE, A. R., WOOD, J. N., DE
5 KONINCK, Y., RIBEIRO-DA-SILVA, A., MOGIL, J. S. & SEGUELA, P. 2013. Remote optogenetic
6 activation and sensitization of pain pathways in freely moving mice. *J Neurosci*, 33, 18631-40.
- 7 DEISSEROTH, K. 2015. Optogenetics: 10 years of microbial opsins in neuroscience. *Nat Neurosci*, 18, 1213-
8 25.
- 9 FAN, B. & LI, W. 2015. Miniaturized optogenetic neural implants: a review. *Lab Chip*, 15, 3838-55.
- 10 FENNO, L., YIZHAR, O. & DEISSEROTH, K. 2011. The development and application of optogenetics. *Annu*
11 *Rev Neurosci*, 34, 389-412.
- 12 ISERI, E. & KUZUM, D. 2017. Implantable optoelectronic probes for in vivo optogenetics. *J Neural Eng*, 14,
13 031001.
- 14 IYER, S. M., MONTGOMERY, K. L., TOWNE, C., LEE, S. Y., RAMAKRISHNAN, C., DEISSEROTH, K. &
15 DELP, S. L. 2014. Virally mediated optogenetic excitation and inhibition of pain in freely moving
16 nontransgenic mice. *Nat Biotechnol*, 32, 274-8.
- 17 JESCHKE, M. & MOSER, T. 2015. Considering optogenetic stimulation for cochlear implants. *Hear Res*, 322,
18 224-34.
- 19 KIM, T., FOLCHER, M., DOAUD-EL BABA, M. & FUSSENEGGER, M. 2015. A Synthetic Erectile
20 Optogenetic Stimulator Enabling Blue-Light-Inducible Penile Erection. *Angewandte Chemie-*
21 *International Edition*, 54, 5933-5938.
- 22 KLEIN, C., EVRARD, H. C., SHAPCOTT, K. A., HAVERKAMP, S., LOGOTHETIS, N. K. & SCHMID, M.
23 C. 2016. Cell-Targeted Optogenetics and Electrical Microstimulation Reveal the Primate Koniocellular
24 Projection to Supra-granular Visual Cortex. *Neuron*, 90, 143-51.
- 25 L, F. H., CASTELA, I., RUIZ-DEDIEGO, I., OBESO, J. A. & MORATALLA, R. 2017. Striatal activation by
26 optogenetics induces dyskinesias in the 6-hydroxydopamine rat model of Parkinson disease. *Mov*
27 *Disord*, 32, 530-537.
- 28 LISKE, H., QIAN, X., ANIKEEVA, P., DEISSEROTH, K. & DELP, S. 2013. Optical control of neuronal
29 excitation and inhibition using a single opsin protein, ChR2. *Scientific Reports*, 3.
- 30 LLEWELLYN, M. E., THOMPSON, K. R., DEISSEROTH, K. & DELP, S. L. 2010. Orderly recruitment of
31 motor units under optical control in vivo. *Nat Med*, 16, 1161-5.
- 32 MAIMON, B. E., ZORZOS, A. N., BENDELL, R., HARDING, A., FAHMI, M., SRINIVASAN, S.,
33 CALVARESI, P. & HERR, H. M. 2017. Transdermal optogenetic peripheral nerve stimulation. *J*
34 *Neural Eng*, 14, 034002.
- 35 MIYASHITA, T., SHAO, Y. R., CHUNG, J., POURZIA, O. & FELDMAN, D. E. 2013. Long-term
36 channelrhodopsin-2 (ChR2) expression can induce abnormal axonal morphology and targeting in
37 cerebral cortex. *Front Neural Circuits*, 7, 8.
- 38 MONTGOMERY, K. L., IYER, S. M., CHRISTENSEN, A. J., DEISSEROTH, K. & DELP, S. L. 2016. Beyond
39 the brain: Optogenetic control in the spinal cord and peripheral nervous system. *Sci Transl Med*, 8,
40 337rv5.
- 41 MONTGOMERY, K. L., YEH, A. J., HO, J. S., TSAO, V., MOHAN IYER, S., GROSENICK, L., FERENCZI,
42 E. A., TANABE, Y., DEISSEROTH, K., DELP, S. L. & POON, A. S. 2015. Wirelessly powered, fully
43 internal optogenetics for brain, spinal and peripheral circuits in mice. *Nat Methods*, 12, 969-74.
- 44 PARK, S. I., BRENNER, D. S., SHIN, G., MORGAN, C. D., COPITS, B. A., CHUNG, H. U., PULLEN, M. Y.,
45 NOH, K. N., DAVIDSON, S., OH, S. J., YOON, J., JANG, K. I., SAMINENI, V. K., NORMAN, M.,
46 GRAJALES-REYES, J. G., VOGT, S. K., SUNDARAM, S. S., WILSON, K. M., HA, J. S., XU, R.,
47 PAN, T., KIM, T. I., HUANG, Y., MONTANA, M. C., GOLDEN, J. P., BRUCHAS, M. R., GEREAU,
48 R. W. T. & ROGERS, J. A. 2015. Soft, stretchable, fully implantable miniaturized optoelectronic
49 systems for wireless optogenetics. *Nat Biotechnol*, 33, 1280-1286.
- 50 PAWELA, C., DEYOE, E. & PASHAIE, R. 2016. Intracranial Injection of an Optogenetics Viral Vector
51 Followed by Optical Cannula Implantation for Neural Stimulation in Rat Brain Cortex. *Methods Mol*
52 *Biol*, 1408, 227-41.
- 53 PISANELLO, F., MANDELBAUM, G., PISANELLO, M., OLDENBURG, I. A., SILEO, L., MARKOWITZ, J.
54 E., PETERSON, R. E., DELLA PATRIA, A., HAYNES, T. M., EMARA, M. S., SPAGNOLO, B.,
55 DATTA, S. R., DE VITTORIO, M. & SABATINI, B. L. 2017. Dynamic illumination of spatially
56 restricted or large brain volumes via a single tapered optical fiber. *Nat Neurosci*.
- 57 SPARTA, D. R., STAMATAKIS, A. M., PHILLIPS, J. L., HOVELSO, N., VAN ZESSEN, R. & STUBER, G.
58 D. 2011. Construction of implantable optical fibers for long-term optogenetic manipulation of neural
59 circuits. *Nat Protoc*, 7, 12-23.
- 60 STEFFENS, H., DIBAJ, P. & SCHOMBURG, E. D. 2012. In vivo measurement of conduction velocities in
afferent and efferent nerve fibre groups in mice. *Physiol Res*, 61, 203-14.

- 1
2
3
4 TOWNE, C., MONTGOMERY, K. L., IYER, S. M., DEISSEROTH, K. & DELP, S. L. 2013. Optogenetic
5 control of targeted peripheral axons in freely moving animals. *PLoS One*, 8, e72691.
6 WARDEN, M. R., CARDIN, J. A. & DEISSEROTH, K. 2014. Optical neural interfaces. *Annu Rev Biomed Eng*,
7 16, 103-29.
8 WU, F., STARK, E., IM, M., CHO, I. J., YOON, E. S., BUZSAKI, G., WISE, K. D. & YOON, E. 2013. An
9 implantable neural probe with monolithically integrated dielectric waveguide and recording electrodes
10 for optogenetics applications. *J Neural Eng*, 10, 056012.
11 YIZHAR, O., FENNO, L. E., DAVIDSON, T. J., MOGRI, M. & DEISSEROTH, K. 2011. Optogenetics in
12 neural systems. *Neuron*, 71, 9-34.
13
14
15
16
17

18 **Supplementary Materials**

19

20
21 **Video V1:** Single-shot optogenetic stimulation of sciatic nerve axons with the behaving mouse
22 sampled at 1 kHz.
23
24
25
26
27
28
29
30
31
32
33
34
35
36
37
38
39
40
41
42
43
44
45
46
47
48
49
50
51
52
53
54
55
56
57
58
59
60